Compact Focusing System for Ion and Electron Beams*

J. Reijonen[i], Q. Ji[ii], T.-J. King[ii], K. N. Leung[iii], A. Persaud and S. Wilde
Lawrence Berkeley National Laboratory, University of California, Berkeley, CA 94720

Abstract

A compact ion and electron beam focusing column design has been developed in Plasma and Ion Source Technology Group in Lawrence Berkeley National Laboratory. The electrostatic ion beam-focusing column was simulated using 2D IGUN[1] ion extraction and beam transport code. A new method has been developed to include finite ion temperature to the IGUN simulation[2]. The focused ion beam system includes an ion temperature collimator, which eliminates the large angle beam trajectories resulting in a small beam spot size. The small holes in the column electrodes are laser-drilled, and are aligned by an optical comparator. Simulations show that focused beam spot size as small as 147 nm is achievable for a 40 keV argon beam. The compact electron beam focusing system consists of three elements: the plasma cathode, an electron temperature collimator (similar to the ion beam temperature collimator) and the focusing electrode elements. The total length of the system is less than 10 mm. The column design is performed using EGUN, electron beam computation code, and IGUN. Space charge effects as well as the electron temperature are incorporated in the computation. The simulations show that focused beam spot size of 60 nm can be achieved. Both columns use similar type RF-induction plasma generator. P^+, BF_2^+ and O_2^+ ion species production by such source is also demonstrated.

Introduction

High-resolution focused ion beams (FIBs) have been used extensively in the semiconductor industry for many applications such as micro-machining, mask repair, circuit modification and

* *This work is supported by DARPA and the U.S. Department of Energy under contract No. DE-AC03-76SF0098.*
[i] *Email:* jreijonen@lbl.gov
[ii] *Also with the Department of Electrical Engineering and Computer Sciences, University of California, Berkeley, CA 94720.*

failure analysis. The FIB systems consist of an electrostatic accelerator or extractor system and electrostatic focusing part. Compact FIB systems can be used in micro-machining applications like magnetic storage head fabrication. Desirable for these applications is a small beam spot size and comparable large beam currents. Both requirements can be fulfilled by using RF-plasma generator, which incorporates high current densities[3] and very low beam axial energy spread[4]. These plasma generators can produce ions from wide range of gases, from hydrogen to xenon, including phosphorus, boron, oxygen, argon ions etc. Low energy P^+ and BF_2^+ beam can be used in direct ion implantation processes to form shallow p-n junction; low energy O_2^+ beam can be used to selectively oxidize the poly-Si surface and form thin SiO_2 film which can be further used as a hard mask for gate patterning in CMOS device process. These make the multicusp plasma source a promising ion source for maskless, resistless lithography[5]. Similarly the RF-plasma generator can be used as a plasma cathode for electron production. By combining these two focused beam techniques one could build a focused ion beam writer together with electron beam diagnostics in to one compact unit.

1. Compact Focusing Column for Ions

The compact focusing column for ions was designed for heavy ions, for example: Ar^+, Kr^+ and . The beam energy is designed to be in the range of 40 keV–50 keV. The column design principle is based on a small outlet aperture, an ion temperature collimator and a focusing section with fairly large apertures. Using the temperature collimator, the large angle beam trajectories can be filtered out. This leads to an effective reduction of the emittance and to a small beam spot size. Simulations have been done using IGUN simulation code with temperature. When simulating with finite (0.1 eV) ion transverse energy the radius of the beam spot is 147 nm with current of 6.5 μA. The simulation and the emittance plot are shown in the Fig. 1. The column consists of six electrodes: extraction electrode, two collimator electrodes and three large aperture focusing electrodes. The total length of the column is less than 10 mm. The small apertures in the column are commercially

available, laser drilled holed in stainless steel. The column is assembled using optical comparator to ensure the alignment of the setup. A picture of the column is shown in the Fig. 2. The column is currently under testing.

2. Ion source characteristics

One of the advantages of the multicusp plasma ion source is that it can produce variable ion species, such as various noble gases, phosphorus, boron, oxygen etc., which make it a promising ion source for maskless, resistless lithography. Direct doping of the Si wafer with a focused P^+ and BF_2^+ beams eliminate the necessity of the resist, which is conventionally used as a mask in ion implantation. The thin oxide formed by selectively oxidizing the poly-Si surface with the focused O_2^+ beam can be used as a hard mask for the gate patterning in the CMOS device process. No mask or resist is involved in such lithography process.

2.1. P^+ ion beam

A small oven is used to heat up a solid phosphorus sample. The phosphorus vapor is introduced into the multicusp source to generate phosphorus plasma. Fig. 4(a) is the mass spectrum of the phosphorus plasma. Over 90% of the ion species are single charged, atomic P^+. Less than 7% are P_2^+ and P_3^+ and P_4^+ combined is less than 1%. In the mass spectrum, the peak of Ar^+ is due to the residue argon gas in the source. Argon is used as a start-up gas before phosphorus vapor is injected into the source chamber. After phosphorus injection the argon gas in the source is been pumped away.

A 5 keV phosphorus beam is implanted into a p-type silicon wafer. After implantation, the sample is annealed at 975°C for 10 sec. As shown in Fig. 4(b), Rutherford Backscattering Spectrum analysis for both as-implanted and annealed samples have been performed. Integrating thee phosphorus peak, the dose of doped phosphorus is $1.3\times10^{16}\,cm^{-2}$.

2.2. BF_2^+ ion beam

Fig. 5(a) is the mass spectrum of BF_3 plasma. B^+, $BF^+$and BF_2^+ ions are generated. Compared to BF^+ and BF_2^+ ions, the amount of the B^+ ions is very small. The plot shown in Fig. 5(b) is the relationship between the BF_2^+ ion percentage and the source power and the BF_3 neutral gas pressure. The BF_2^+ ion percentage increases with the increasing gas pressure, and decreases with the source power. By optimizing these two source parameters, the purity of over 85% of the BF_2^+ ions can be achieved as shown in Fig. 5(a).

2.3. *O_2^+ ion beam:*

Fig. 6 is the mass spectrum of the oxygen plasma. Two ion species are produced: O^+ and O_2^+. The percentage of O_2^+ ions can be optimized by adjusting the source operation parameters, like neutral gas pressure and discharge power, similarly to the BF_2^+ production. By increasing the oxygen gas pressure, decreasing the RF power, and decreasing the gap between RF quartz antenna and the extraction aperture, the percentage of O_2^+ increases. Over 90% of O_2^+ can be achieved.

3. Electron Beam Focusing Column

The design for the compact focused ion beam column can also be used to focus an electron beam. To achieve this, one has to apply positive voltages to the extraction electrode and the focusing system. Optimization of the focusing system was obtained using the computation codes EGUN and IGUN, which includes space charge effect. Fig. 7 (b) shows the design for the focusing system and the applied voltages. The emittance of the beam at the focus point is shown in Fig. 7(a). The normalized 4 RMS emittance is 1.5×10^{-4} π-mm-mRad, the normalized 100% - emittance is bigger by a factor of three. In the simulation a beam spot size of 60 nm in radius can be achieved. For the computation a plasma-density of 5×10^{10} cm^{-3} was assumed, which leads to an electron current of 3.3 μA at the focus point. During the beam transport (especial at the temperature collimator) a current loss of 25 μA occurs. At the focus point a beam current density of 30 kA/cm^2 can be obtained. Furthermore simulations show that changing the voltages at the focusing system can vary the position of the focus point (± 1mm) without changing the size of the focus point.

One advantage of using a plasma source is the uniformity of the beam. Multiple beams can be formed using a mask at the extraction aperture or shortly behind it. Another way to produce multiple beams is to use field emitters. A possible problem using this approach is the alignment of the emitter tips. Normally many field emitters are generated on the same plane, but if the tips of two of these emitters are misaligned by for example one degree, our computation (Fig.8) shows that you can have a large displacement of the beam spot. Furthermore there is going to be a large emittance grows and therefore the brightness of the beam reduces (Fig 9). This problem does not occur if one uses a plasma cathode. For the simulation of a field emitter the computer code SIMION was used. The results of this simulation only give a qualitative result, since no attempt to optimize the geometry for the field emitter was made.

Summary

In summary, a compact ion beam focusing system was designed for micro-machining application. Simulation shows that approximately 150 nm beam spot size can be achieved at the target. Simulations included the use of the finite ion transverse energy. Since the multicusp plasma ion source is capable of producing variable ion species, the similar techniques can be easily applied to maskless, resistless lithography area. Also a 60 nm in radius focused electron beam from a plasma cathode has been investigated. Incorporating a focused electron beam column, which geometry is similar to the focused ion beam column, to a focused ion beam column a compact system can be build which not only include the focused ion beam writer but also focused electron beam system for diagnostics. This type of set-up is shown in Fig. 10.

---

1 R. Becker and W. B. Herrmannsfeldt, *Rev. Sci. Intrum.* 63, 2756 (1992)

2 J. Reijonen, R. Thomae, R. Keller, Proceedings LINAC Conference 2000

3 J. Reijonen, M. Eardley, R. Keller, J. Kwan, K. N. Leung, D. Pickard, R. Thomae and M. D. Williams, Proceedings PAC Conference 1999

4 Y. Y. Lee *et al*., *Nucl. Instr. And Meth. in Phys. Res.* **A**, **374**, 1 (1996)

5 Q.Ji, T.-J. King, K. N. Leung, S. B. Wilde, ICIS 2001. (submitted)

List of Figures:

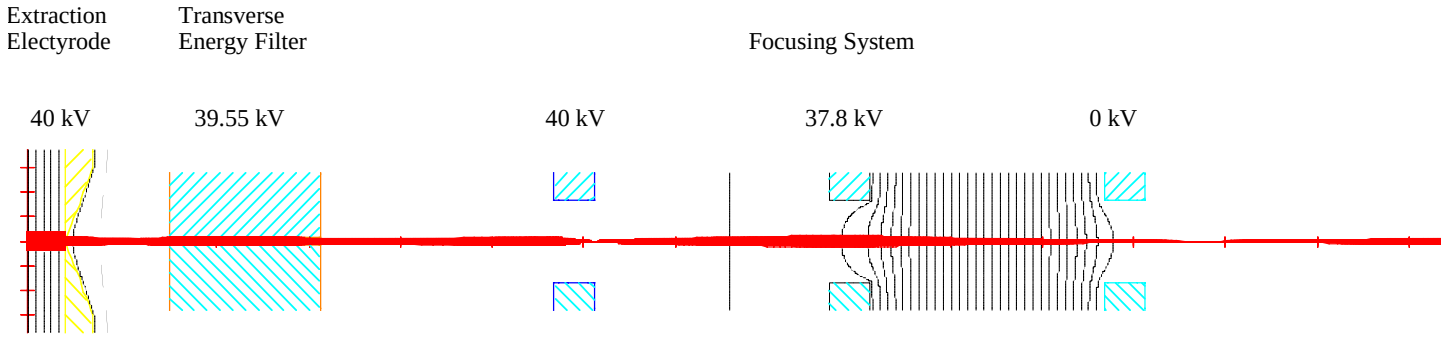
Extraction
Electyrode
Transverse
Energy Filter
Focusing System
40 kV
39.55 kV
40 kV
37.8 kV
0 kV

FIG. 1

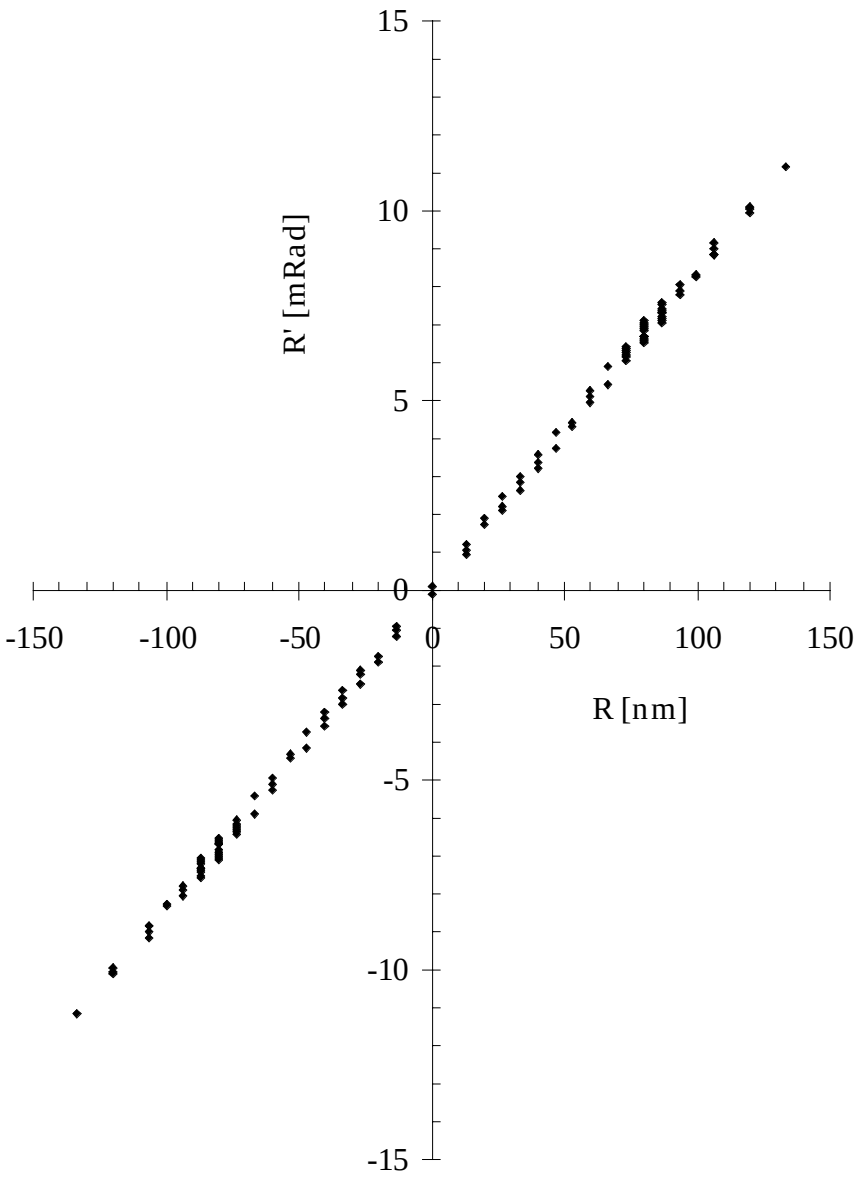

FIG. 2.

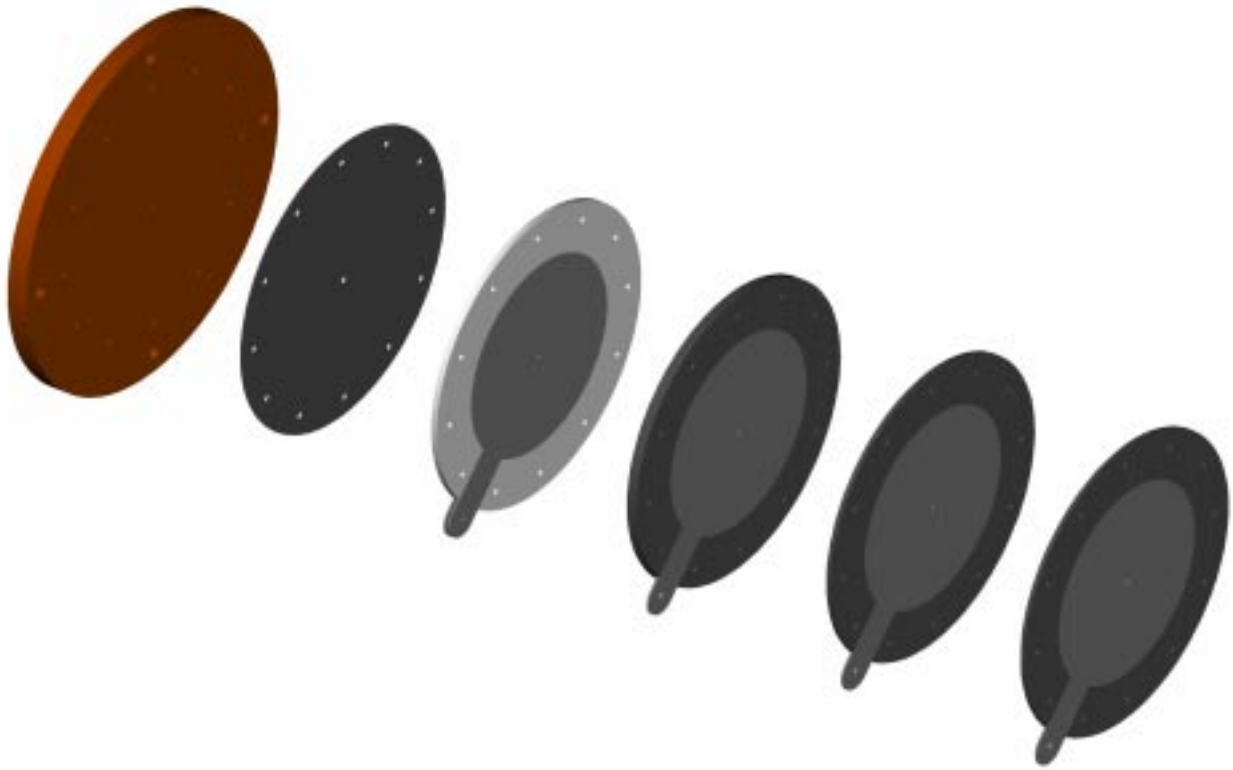

FIG. 3.

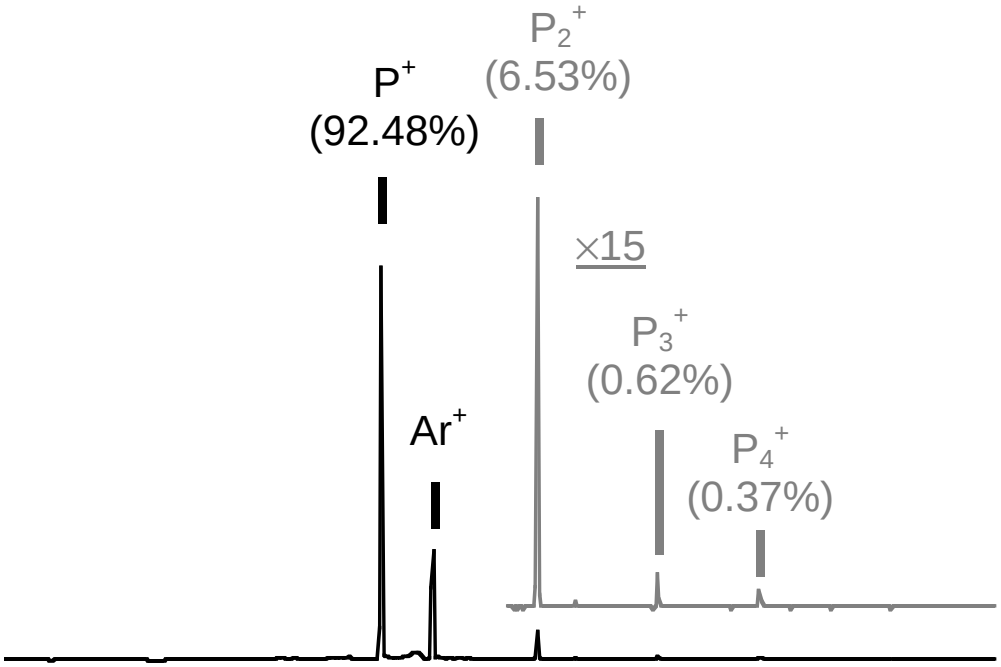

(a)

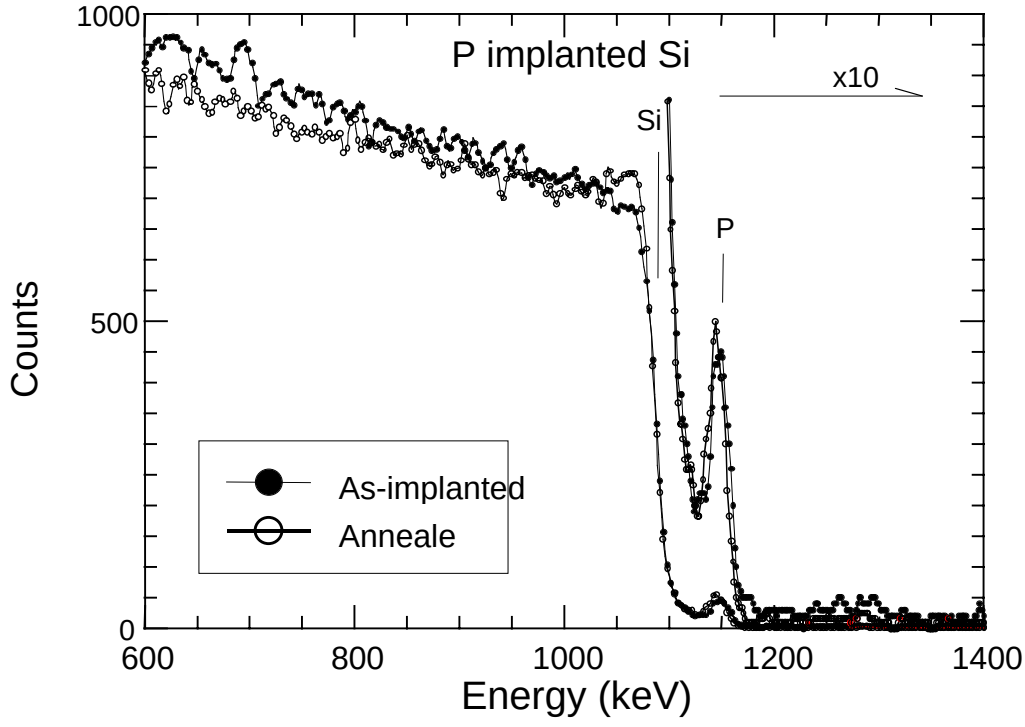

(b)

Fig. 4. (a) Mass spectrum of phosphorus plasma.
(b) Rutherford backscattering spectrum of as-implanted and annealed Si wafer after doped with 5 keV P+ ion beam.

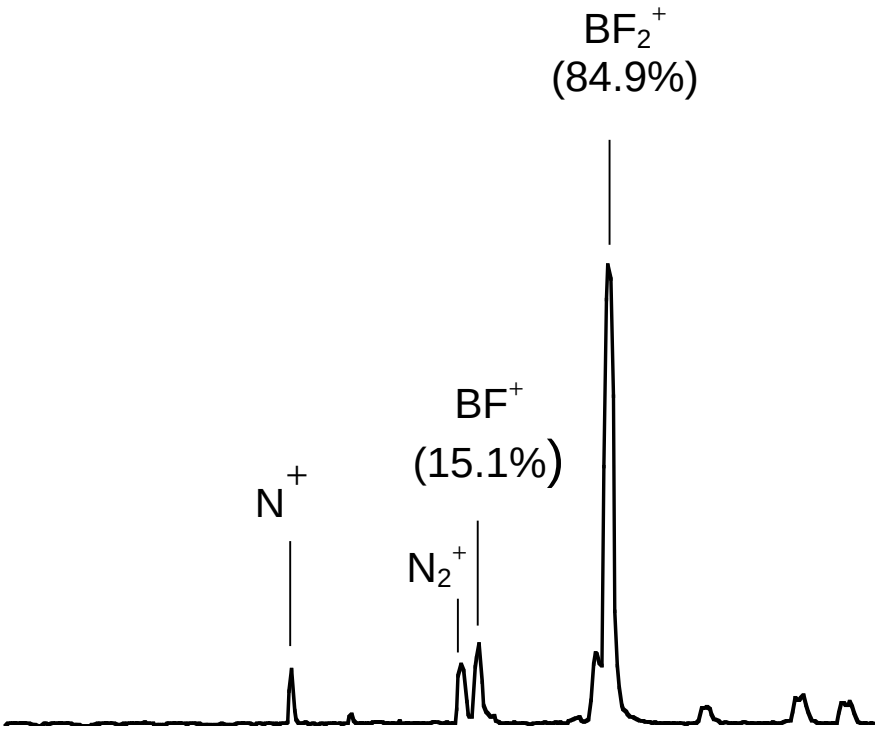

(a)

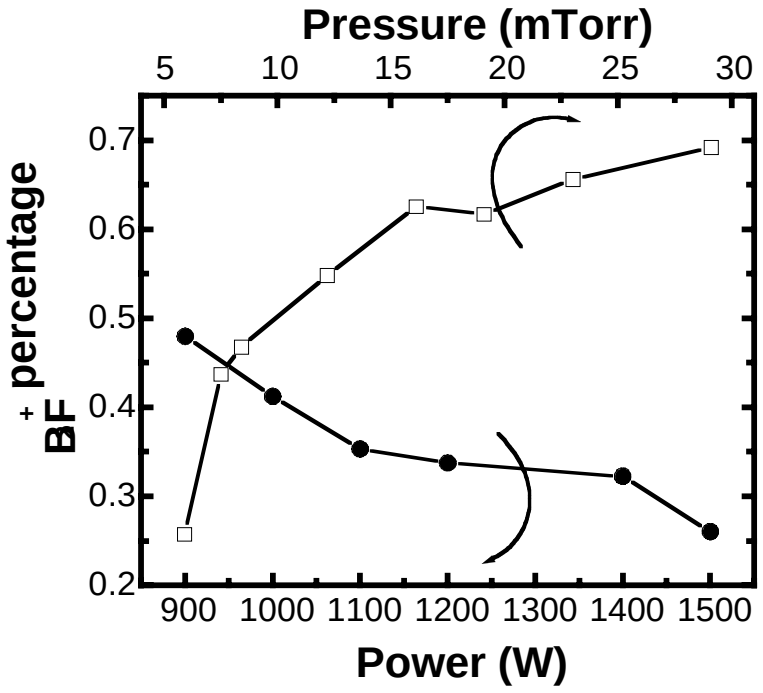

(b)

Fig. 5. (a) Mass spectrum of BF_3 plasma.
(b) RF power and BF_3 gas pressure dependence for BF_2^+ ion production.

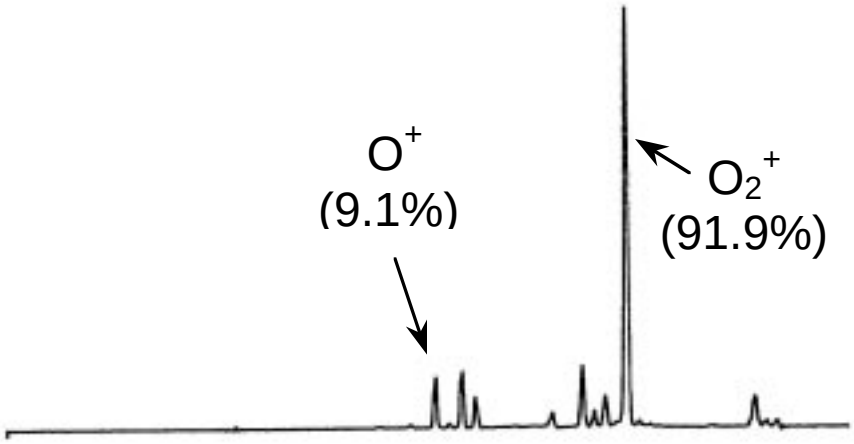

Fig. 6. Mass spectrum of O_2 plasma.

A)

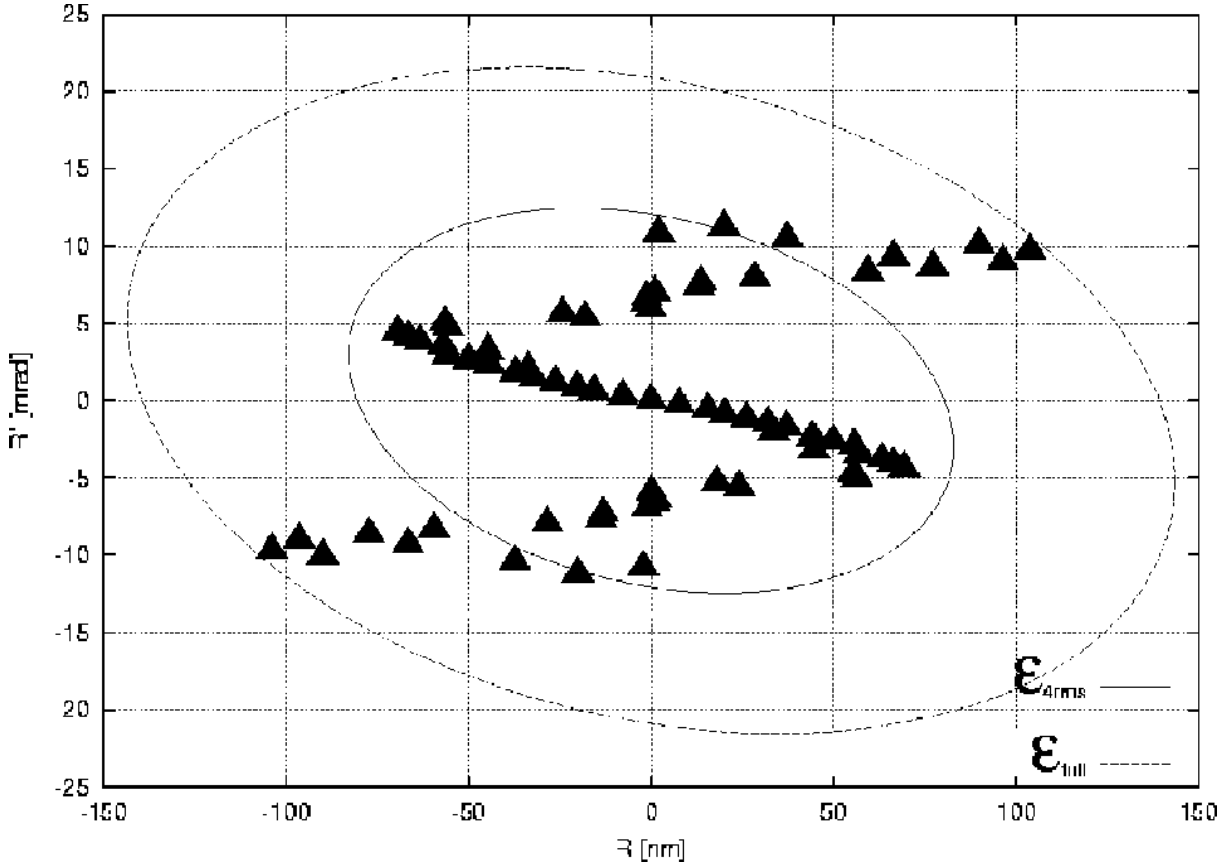

B)

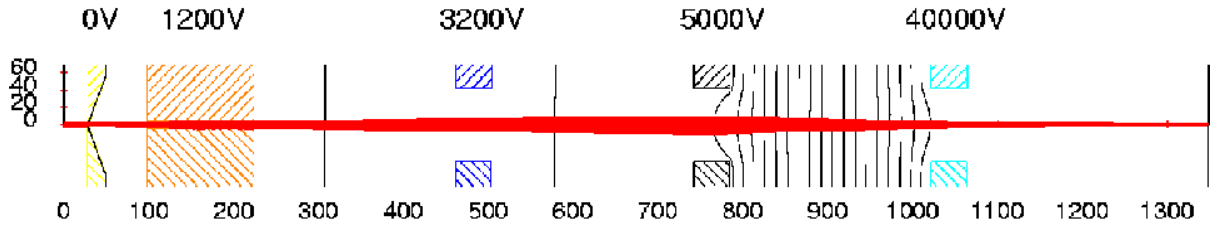

Fig. 7. (a) Emittance of the electron beam at the focus point
(b) Geometry and applied voltages for the focused electron beam column

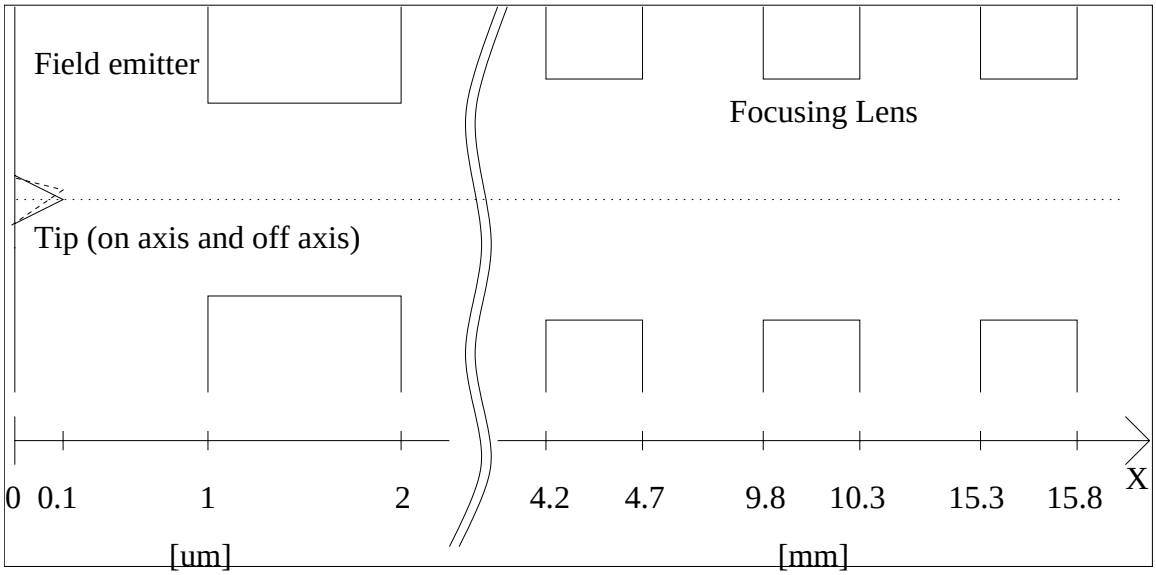

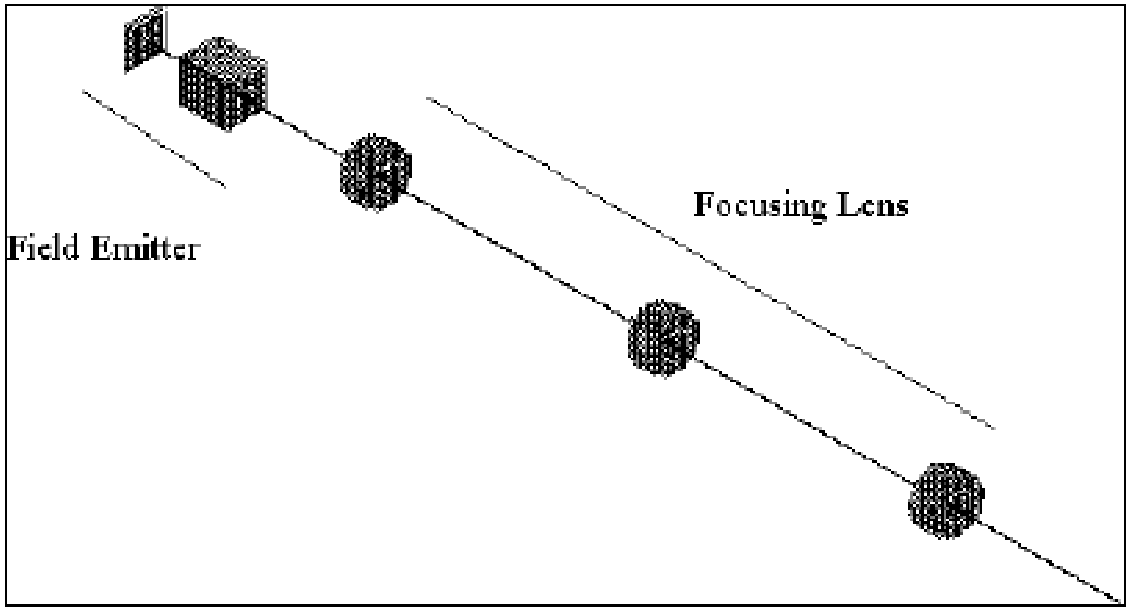

Fig. 8. Geometry used for the simulation of a field emitter

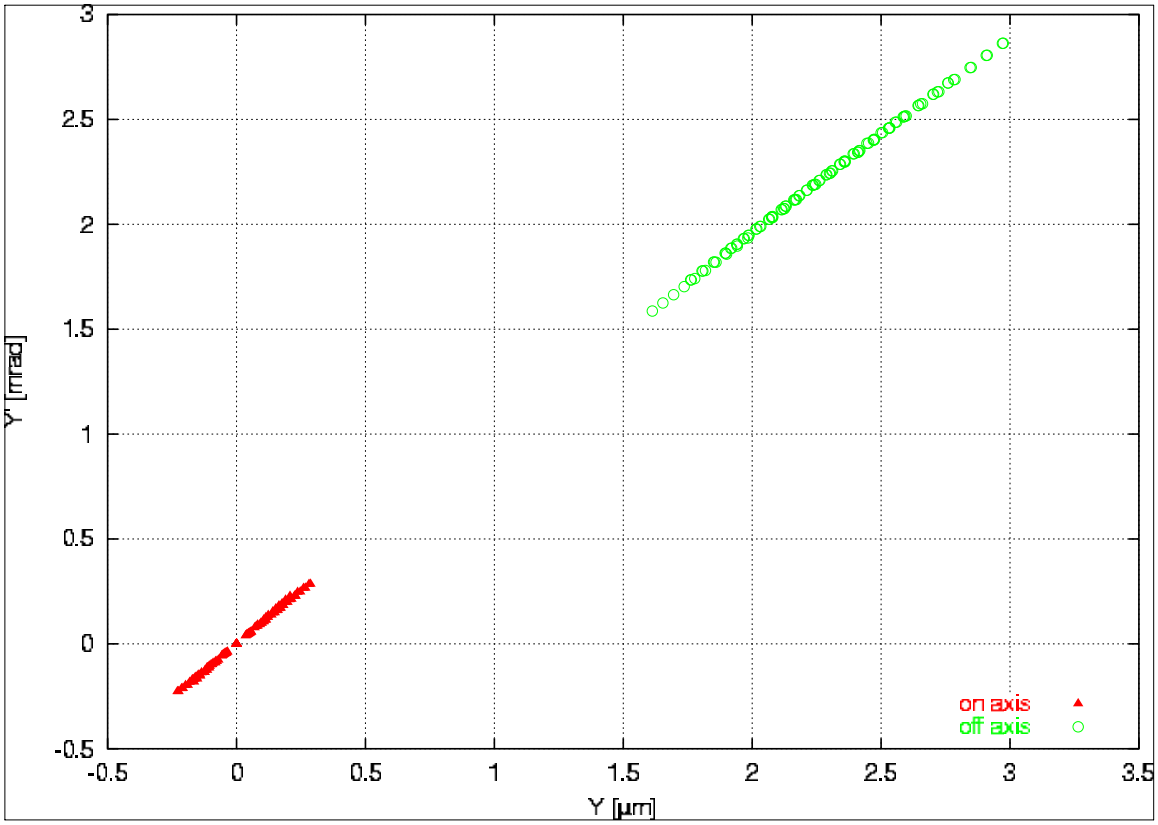

Fig. 9. Emittance plot for a perfect aligned field emitter and a field emitter tip, which is misplaced by an angle of one degree.

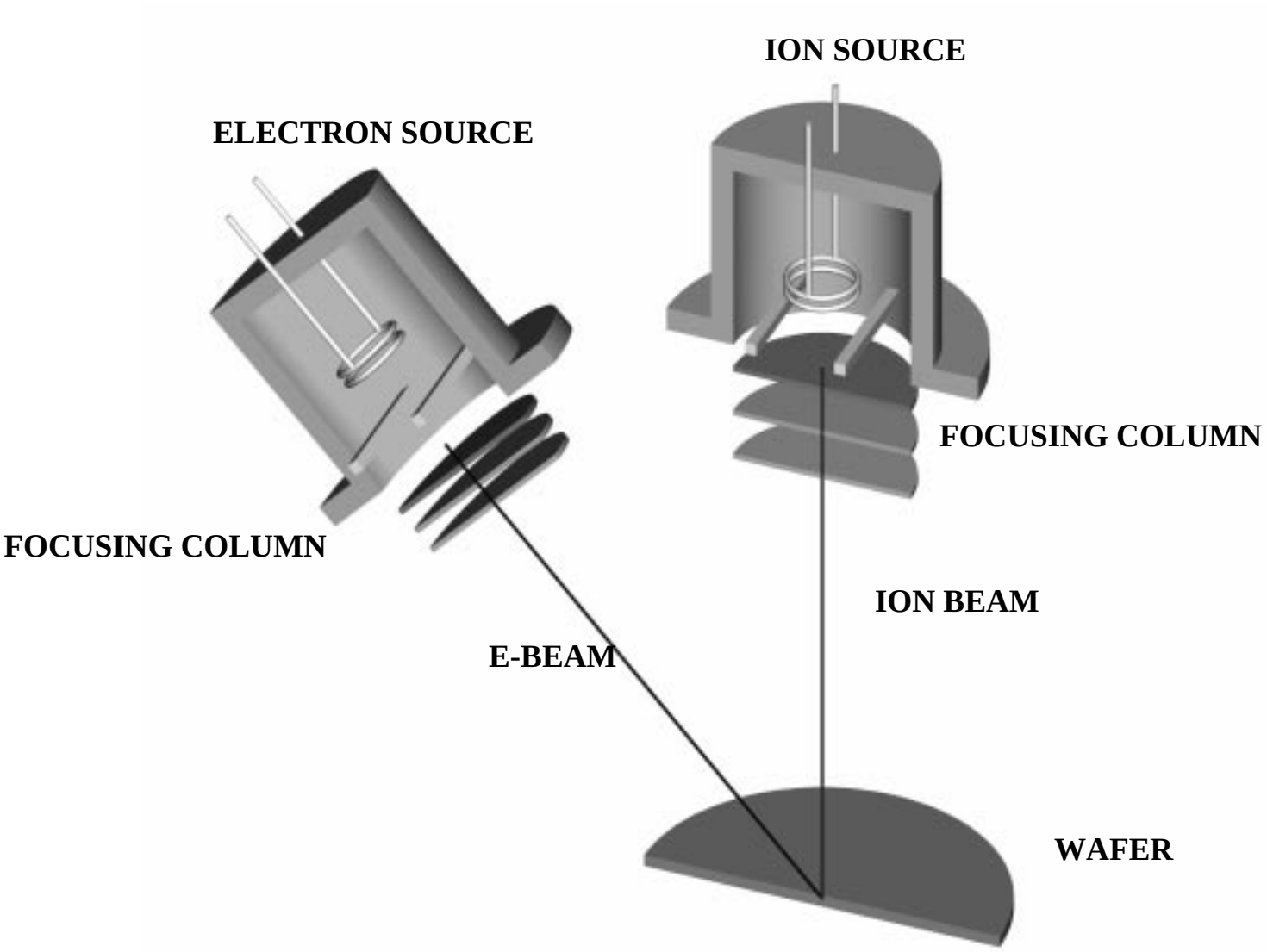

FIG. 10. Combined compact electron and ion beam focusing column for ion beam writing and on-line electron beam diagnostics.